Polydimethylsiloxane-Embedded Conductive Fabric: Characterization and Application for Realization of Robust Passive and Active Flexible Wearable Antennas

ROY B. V. B. SIMORANGKIR[ID]**1, (Student Member, IEEE),**
YANG YANG[ID]**2, (Senior Member, IEEE), RAHEEL M. HASHMI**[ID]**1, (Member, IEEE),**
TONI BJÖRNINEN[ID]**3, (Senior Member, IEEE), KARU P. ESSELLE**[ID]**1, (Fellow, IEEE),**
AND LEENA UKKONEN[3]**, (Member, IEEE)**

[1]School of Engineering, Macquarie University, Sydney, NSW 2109, Australia
[2]School of Electrical and Data Engineering, University of Technology Sydney, Ultimo, Sydney, NSW 2007, Australia
[3]BioMediTech Institute and Faculty of Biomedical Sciences and Engineering, Tampere University of Technology, 33720 Tampere, Finland

Corresponding author: Roy B. V. B. Simorangkir (roy.simorangkir@mq.edu.au)

ABSTRACT We present our study on polydimethylsiloxane (PDMS)-embedded conductive fabric, which we propose as a simple yet effective solution to the challenging issue of poor PDMS-metal adhesion, allowing for a relatively easy realization of robust flexible antennas for wearable applications. The method combines the use of conductive fabric as a radiator with PDMS, which acts as the substrate and a protective encapsulation simultaneously. For the first time, a holistic study on the mechanical and electrical properties of the proposed combination of materials is presented thoroughly using a number of fabricated samples. As concept demonstrations, a microstrip patch and a reconfigurable patch antenna are fabricated using the proposed technique to validate the idea. The inclusion of a PDMS-ceramic composite as part of the antenna's substrate, which leads to over 50% reduction in the size compared with a pure PDMS, is also demonstrated to showcase further the versatility of the proposed technique. The fabricated antennas are tested in several wearable scenarios and consistent performance including reconfigurability is obtained even after the antennas are exposed to harsh environments, i.e., extreme bending and machine-washing.

INDEX TERMS Conductive fabric, flexible antenna, frequency-reconfigurable antenna, patch antenna, polydimethylsiloxane (PDMS), polymer-ceramics composite, reconfigurable, varactors, wearable.

I. INTRODUCTION

The emerging wearable wireless communication has created an increasing demand for a flexible, reversibly deformable, and wearable antenna as the key component in the Radio Frequency (RF) front-end of the system. Considering the necessity of comfort for prolonged use, conventional antennas fabricated using rigid PCB technology are not suitable for this application. This is due to their poor flexibility, thus not allowing them to cope with the dynamics of the human body and to stand mechanical deformations in the human body environment, such as bending, twisting, and stretching.

To address this major limitation, significant efforts have been focused on the realization of flexible wearable antennas using unconventional materials [1]–[29]. Among these, the use of polydimethylsiloxane (PDMS) polymer has been emerging as one of the most promising approaches. That is due to their remarkably low Young's modulus (< 3 MPa), indicating an extremely high flexibility/conformality compared to any other polymers [30], [31] and an acceptable loss in the microwave region with an easy-to-tune relative permittivity value [1]. In addition to a low-cost preparation [3] and versatile fabrication process due to its initial liquid state [10], the molecular structure of PDMS renders its unique properties of water-resistance, heat-resistance (up to 400°C), UV-rays resistance, and chemical stability, making PDMS resilient to extreme environments [32], [33].

With such benefits, the inherently weak metal-polymer adhesion [34] nevertheless challenges the development of flexible antennas with PDMS. Any common metal deposition techniques or direct attachment of metal sheet generally do not work well for PDMS [3], [4], [34], causing the integration of the antenna conductive parts particularly problematic. A poor metal-polymer adhesion can lead to frequent detachment of the antenna conductive parts under deformation and stress, and hence compromise the antenna's RF performance. In the last decade, some solutions to this issue have been proposed, which include embedding carbon nanotube sheets [3], embedding perforated copper sheet [10], embedding silver nanowires (AgNWs) [12], [21], injecting liquid metal [35], and oxygen plasma treatment on the PDMS surface prior to metal deposition [20], [34], [36]. Generally, the primary issue with these approaches is the complexity of the fabrication process, whereas the properties of materials, such as the low conductivity of the carbon nanotube [37], the possibility of liquid metal leakage [12], the less flexibility and durability of copper sheet (i.e. possibilities of cracks or permanent folds after extreme strains) [35], and the high material cost of silver [24] are some of the several secondary challenges. On the other hand, the method of embedding embroidered conductive threads has also been proposed in [38] and [39]. However, the application has only been demonstrated for wire type antenna where the surface contact between the conductive part and the PDMS is very minimum.

In this paper, we present PDMS-embedded conductive fabric as a simple yet effective approach to overcome the challenge of poor PDMS-metal adhesion, allowing for a relatively easy realization of flexible and mechanically robust PDMS-based wearable antennas. We also performed a thorough characterization of the mechanical and electrical properties of this method using four potential combinations of PDMS-embedded conductive fabric. This characterization process provides insight into the mechanical robustness of this approach, the constraints associated with selection of the conductive fabric for various parts of the antenna, and the effective modeling of the antenna, which is valuable in the design process of the antenna. To the best of the authors' knowledge, this has never been explored previously in any related works [38], [39] including our first presentation of this technique [28]. Based on those studies, using the most suitable combination, we design and fabricate flexible antenna examples, including a reconfigurable antenna, as concept demonstrations. We also expand the PDMS-conductive fabric combination by incorporating a PDMS-ceramic composite substrate which leads to a more than 50% reduction of antenna size without compromising the antenna flexibility, robustness or RF performance, as compared to the one using pure PDMS in [28]. To validate the robustness provided by the proposed approach, the performance of the antennas is studied by subjecting them to various extreme environments such as extreme bending and machine-washing.

Compared to previously reported approaches in [4], [5], [22], and [25], that utilize similar combinations of materials,

TABLE 1. Conductive fabrics investigated in this work.

Type	Composition	t (mm)	σ (S/m)
CF I	nickel-copper-silver coated nylon ripstop	0.13	7.7×10^5
CF II	copper coated polyester taffeta	0.08	2.5×10^5
CF III	nickel-copper coated ripstop	0.08	4.2×10^5
CF IV	silver coated ripstop	0.05	8×10^4

Note: t = thickness, σ = effective conductivity

by merely attaching the conductive fabric or embroidered layers on the surface of the PDMS, a significantly stronger integration is achieved that leads to their withstanding very harsh operating conditions. The full encapsulation by PDMS provides the physical robustness needed by wearable applications as it keeps all the antenna parts in place, avoids detachment even under severe deformation, and protects them from harsh environments. Therefore, this approach is also suitable for implementation of robust active wearable antennas, whose performance can be tuned by means of electronic tuning components attached to the body of the antenna.

II. CHARACTERISTICS OF PDMS-EMBEDDED CONDUCTIVE FABRIC

A. MATERIALS

As the conductive elements, only woven conductive fabric is considered in this work for its higher and more isotropic effective conductivity, compared to that of knitted conductive fabric [2]. Among the available conductive fabrics, we chose the four woven conductive fabrics, CF I, II, III, and IV, listed in Table 1. Specifically, these fabrics are composed of entirely plated multifilament threads intertwine with each other in a one-to-one ratio between the vertical and horizontal directions. The distance between adjacent groups of threads is very small, less than 0.04 mm, thus allowing a good resemblance to a solid metallic plate [11]. The information about the fabrics was gathered from the datasheets provided by the manufacturers, Marktek Inc. and Less EMF Inc. The major differences between the fabrics are their thicknesses, the composition of the metal coating on the threads, and the threads density, which lead to different effective conductivities, affecting the performance of the fabricated antenna.

On the other hand, for the non-conductive elements, we prepared two different types of polymers: (a) pure PDMS, and (b) PDMS-ceramic composite polymer. To make the PDMS layers, a solution prepared using a Dow Corning Sylgard 184 silicone elastomer kit through the process described in [5] was used. The PDMS-ceramic composite was prepared by mixing the PDMS solution with 20% volume of $SrTiO_3$ ceramic powder, which will be applied later during the antenna demonstrations in Section III. $SrTiO_3$ is well known for its very high relative permittivity of 270 and a low loss tangent below 0.001 at microwave frequencies [40], [41]. The electrical properties of the solutions are shown in Figs. 1(a) and (b), which were obtained through measurements using an Agilent 85070E Dielectric Probe Kit. It is
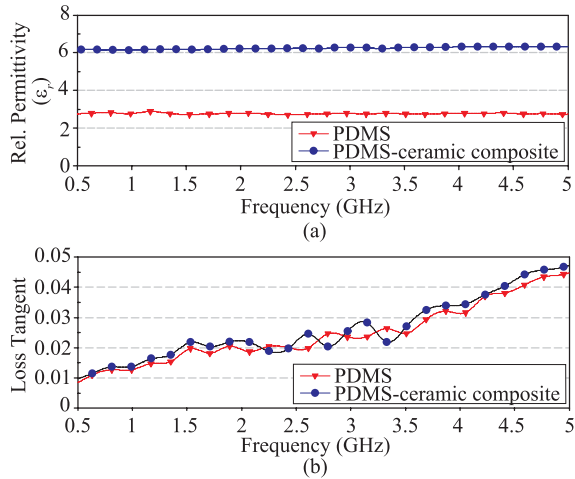
FIGURE 1. Measured electrical properties of PDMS and PDMS-ceramic composite with 20% volume of SrTiO$_3$ loading. (a) Relative permittivity. (b) Loss tangent.
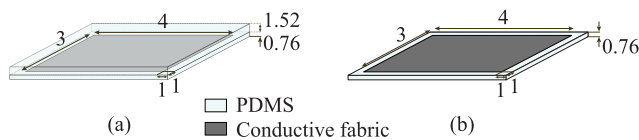

FIGURE 2. Illustration of the samples. (a) When the conductive fabric is embedded inside the PDMS. (b) When the conductive fabric is simply attached on the PDMS surface. All dimensions are in millimeters.

interesting to note in Fig. 1 that the PDMS-ceramic composite provides nearly twice the permittivity of the pure PDMS with a reasonably similar loss characteristic. This property is used in Section III to achieve significant miniaturization of the antenna.

B. MECHANICAL CHARACTERIZATION

To investigate the mechanical properties of the PDMS-embedded conductive fabric, we fabricated four samples out of four different conductive fabrics. For validation purposes, three prototypes were made for each type of sample, which all have the same dimensions as depicted in Fig. 2(a). To highlight the advantage of this approach compared with previously reported works, where the conductive fabrics/embroidered layers were attached on the surface of the PDMS substrate [4], [5], [22], [25], the non-encapsulation-layer version of all samples were also prepared as illustrated in Fig. 2(b). For mechanical characterization, we utilize only pure PDMS considering that the addition of 20% volume of SrTiO$_3$ does not change the nature of metal-PDMS adhesion.

As illustrated in Fig. 3(a), all of the samples were subjected to a set of mechanical stress testings including severe rolling, twisting, and bending, each repeated 50 times. The tests were conducted in two cycles, and comparisons between the samples before and after each testing cycle are given in Figs. 3(b) and (c). The results show that the PDMS-embedded conductive-fabric approach provides a significantly improved physical robustness compared to the previous method of
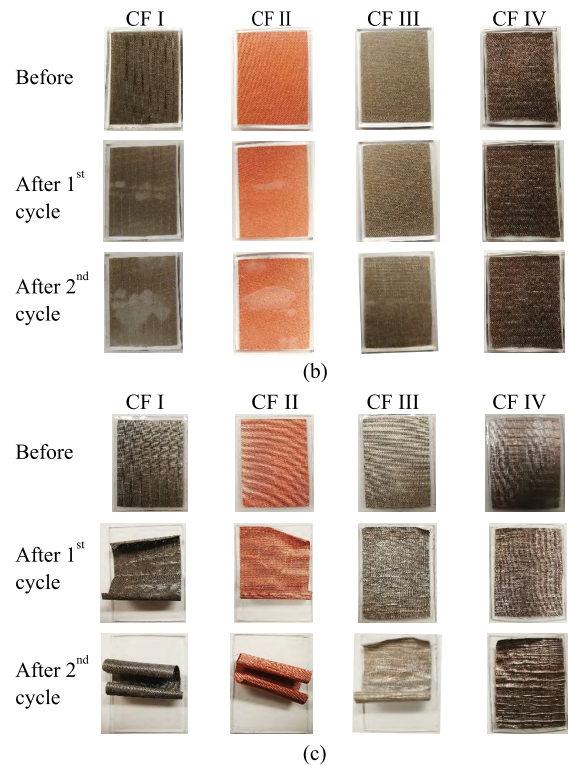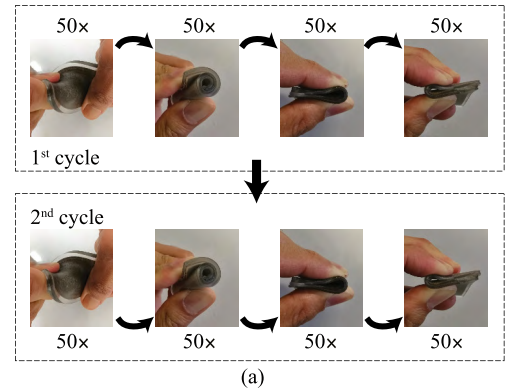

FIGURE 3. (a) Illustration of mechanical testing scenarios. Photograph of the samples before and after tests, when: (b) the conductive fabric is embedded inside the PDMS layer; (c) the conductive fabric is simply attached on top of the PDMS layer.

attaching the conductive fabric on the surface of a PDMS layer. During the tests, we observed that without the PDMS encapsulation layer a possibility of the fabric to detach from the substrate, often starting from the edge and expanding further to the whole part of the fabric, is still very high, resulting in what is shown in Fig. 3(c). These results also indicate that samples fabricated with the previous method may not endure washing.

C. MECHANICAL STABILITY DUE TO STRUCTURAL CHARACTERISTICS OF PDMS-EMBEDDED CONDUCTIVE FABRIC

Let us study the physical structure of the PDMS-embedded conductive fabric by observing it under the scanning electron
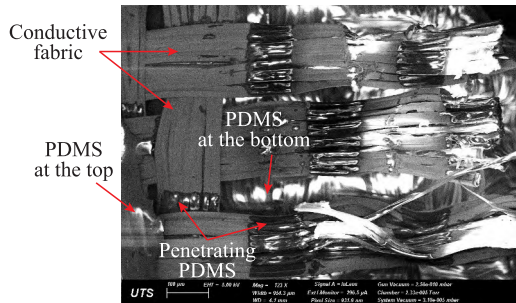
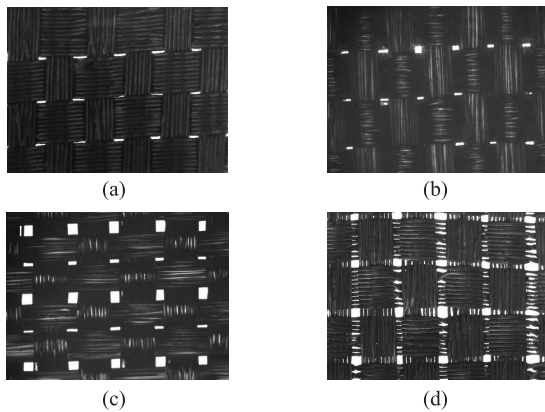**FIGURE 4.** SEM image view of a PDMS-embedded conductive fabric sample.

FIGURE 5. Photograph of the conductive fabric under a fluorescence microscope. (a) CF I. (b) CF II. (c) CF III. (d) CF IV.

FIGURE 6. PDMS-embedded conductive-fabric transmission lines. (a) Design (All dimensions are in millimeters). (b) Photograph of the fabricated prototypes.
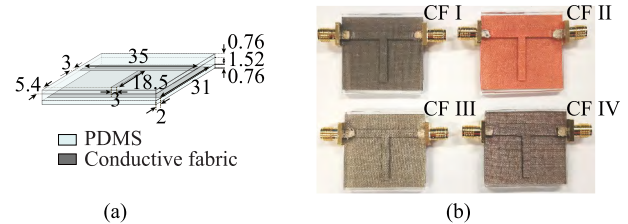

FIGURE 7. PDMS-embedded conductive fabric T-resonators. (a) Design (All dimensions are in millimetres). (b) Photograph of the fabricated resonators.

microscope (SEM), a snapshot for which is shown in Fig. 4. A typical conductive fabric consists of multifilament conductive yarns intertwining with each other, leaving a porous conductive surface. This allows the PDMS in its initial liquid form to penetrate through the conductive fabric and bond with the PDMS encapsulation layer on the other side of the conductive fabric. Normally, the adhesion between PDMS and the conductive elements like metals is weak [4], [34]. However, with the extra support from the PDMS-PDMS layer adhesion which is much stronger than that of the PDMS and conductive fabric, better structural integration is obtained, thus allowing the structure to stand against severe deformations better.

As an implication, the mechanical stability of the PDMS-embedded conductive fabric depends upon the porosity of the conductive fabric as it determines the amount of PDMS-PDMS layers bonding that can be achieved across the fabric. In Figs. 5(a)–(d) photos of the four conductive fabrics under a fluorescence microscope with ten times magnification are given. The figures show an increasing porosity from CF I to CF IV. This explains the mechanical testing results in Fig. 3(b), where the mechanical robustness of the sample increases from CF I to CF IV. It is determined by the amount of white mark across the samples that decreases from CF I to CF IV. The white mark indicates the gap formed between the conductive fabric and PDMS due to repeated

severe deformations. Although for some combinations the gap can still appear, it is worth noting that in this approach the conductive fabric still retains its electrical connectivity as it does not suffer from the crack formation as in a flexible PCB substrate under severe bending. Moreover, in contrast to the samples fabricated with previous methods (Fig. 3(c)), the conductive fabric remains inside the PDMS layer, thus is still protected from being peeled off or washed away.

D. ELECTRICAL PROPERTIES OF PDMS-EMBEDDED CONDUCTIVE FABRIC

To characterize the electrical properties of the PDMS-embedded conductive fabric, we fabricated and measured the performance of four 50 Ω microstrip transmission lines with dimensions shown in Fig. 6(a). The fabricated prototypes are shown in Fig. 6(b). Additional loss in the conductive part was observed, likely contributed by PDMS penetration into the conductive fabric, and therefore needs to be considered during the simulation to attain an accurate design. To do that, the effective conductivity of the conductive fabric which was modelled in CST Microwave Studio 2016 using a box with the fabric thickness was adjusted in the simulation, until the best match between the simulated and measured |*S*|-parameters was achieved [42]. For validation, the values were also evaluated using the T-resonators [43] shown in Figs. 7(a) and (b), designed and fabricated using the same combinations of PDMS-embedded conductive fabric. The effective conductivity was readjusted until the resonance in simulation matches well with that of the measurement, as shown in Figs. 8(a)–(d).

The comparison between the simulated and measured |*S*|-parameters of the transmission lines after adjusting the effective conductivity value is shown in Figs. 9(a) and (b). For all prototypes the return loss is above 16 dB over the whole
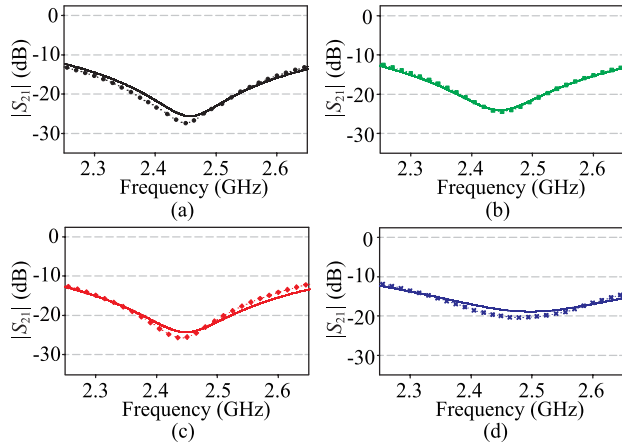
FIGURE 8. Simulated (solid lines) and measured (dotted lines) transmission coefficient ($|S_{21}|$) of PDMS-embedded conductive fabric T-resonators with (a) CF I, (b) CF II, (c) CF III, and (d) CF IV.
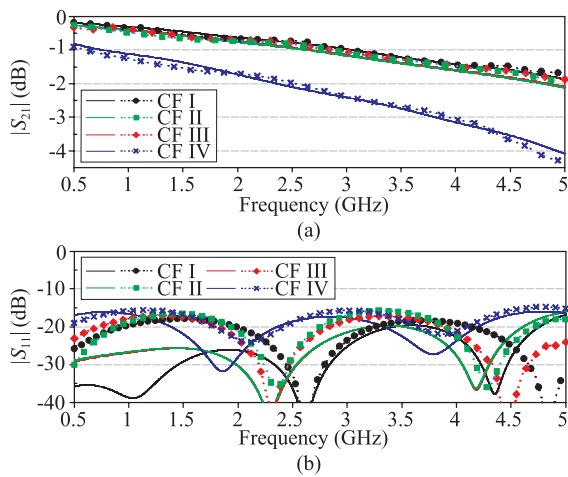

FIGURE 9. Simulated (solid lines) and measured (dotted lines) $|S|$-parameters of the fabricated transmission lines. (a) $|S_{21}|$. (b) Input reflection coefficient ($|S_{11}|$).

TABLE 2. Estimated conductivities used to model the conductive fabrics embedded in PDMS.

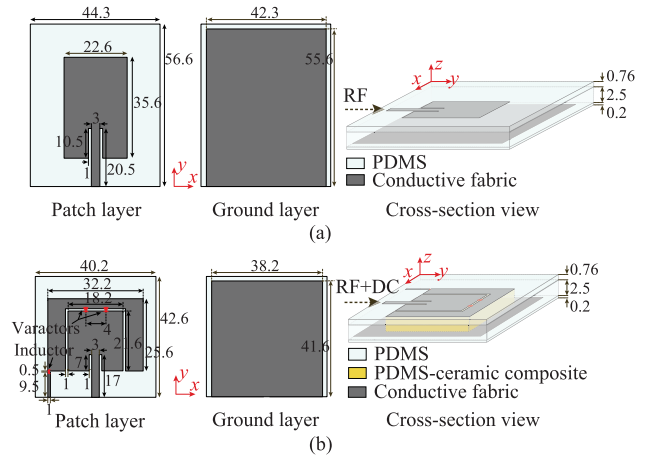| Conductive Fabric Type	Estimated σ (S/m)
CF I	1.02×10^5
CF II	5×10^4
CF III	5.4×10^4
CF IV	4.8×10^3

Note: σ = effective conductivity

FIGURE 10. Antennas designed for concept demonstrations. (a) PA. (b) RFPA. All dimensions are in millimeters.

observation band, and as expected the insertion loss varies, indicating the different conductivity of each conductive fabric used. The adjusted conductivity values, which are lower than those of the plain conductive fabric provided in the datasheet, are given in Table 2. These are the values which were applied to model the conductive fabric embedded in PDMS during the antenna design stage.

III. PDMS-EMBEDDED CONDUCTIVE FABRIC IN REALIZATION OF WEARABLE ANTENNA

A. PASSIVE AND ACTIVE PATCH ANTENNAS CONFIGURATIONS

To demonstrate the applicability of the proposed approach for realization of robust wearable antennas, as illustrated in Figs. 10(a) and (b), we designed a regular inset-fed rectangular patch antenna operating in ISM 2.45 GHz band together with its active version which has the capability of continuous resonance-frequency tuning. Henceforth, they will be

referred to as PA and RFPA, respectively. PDMS layers are used as the substrate and encapsulation that completely covers the antennas, including the electronic tuning and RF choking components in the RFPA. We also employed the prepared PDMS-ceramic composite as part of the substrate of the RFPA. A full ground plane is maintained in both designs for a low antenna-human-body coupling level which is essential in wearable applications.

The total size of the RFPA was reduced by 52% by loading 20% volume of SrTiO$_3$ ceramic powder in the PDMS polymer, as compared to the pure PDMS embedded antenna demonstrated initially in [28]. This decrease in antenna size results from an increase in the permittivity of the polymer up to 6.36, yet with a marginal change in the loss. This is a significant improvement without compromising the flexibility of the antenna or its performance. The dimension of the composite substrate was optimized to be as large as the area of the radiating patches, after considering the miniaturization factor and additional dielectric loss contributed by the ceramics. More miniaturization could be achieved by adding more ceramic powder, but at the expense of further dielectric losses and lower fringing fields due to the high permittivity [44]. These two together will degrade the efficiency of the antenna. Moreover, a larger amount of ceramic loading affects the flexibility of PDMS and complicates its fabrication process, as the mixture becomes thicker and thus harder to mix homogeneously [45].

**TABLE 3.** Reverse bias voltage and corresponding varactor junction capacitance.

Bias State	V_1	V_2	V_3
Voltage (V)	0	4	20
C_j (pF)	1.1	0.46	0.097

Apart from the inclusion of PDMS-ceramic composite substrate, the improvement in the RFPA from the one in [28] includes the use of thinner substrate and encapsulation layers to reduce the profile of the antenna further. Moreover, the conductive parts of the antenna were realized using different combinations of conductive fabrics, which leads to a better mechanical robustness. Both in PA and RFPA, the antenna patches were realized with CF I due to its highest conductivity among the other four conductive fabrics, which is necessary for a higher antenna efficiency. On the other hand, considering its high porosity and acceptable conductivity, CF III was chosen over CF IV for the ground plane. Fabric with higher porosity is more beneficial for such a large surface as a ground plane as it minimizes the possibility of fabric detachment.

The continuous frequency reconfigurability is achieved by adding a U-shaped parasitic around the rectangular patch and connecting them using two varactors. The varactors are placed in line with the dominant current path of the rectangular patch operating in its fundamental mode so that the effective electrical length of the patch can be changed through the variation of a DC bias voltage applied to the varactors. The two varactors are reverse biased by a single DC voltage applied to the antenna together with the RF signal, using a bias tee to eliminate the need for a complex bias circuit. The cathodes of the varactors are connected to the rectangular patch, while the anodes are connected to the parasitic patch. The parasitic patch is DC grounded by a thin conducting line which is isolated from the RF signal by an RF-choke chip inductor (47 nH) from Coilcraft. The MGV 125-20-0805-2 varactor diodes from Aeroflex Metelics were chosen for their low parasitic resistance (R_s) and adequate range of junction capacitance (C_j). During the antenna simulation and optimization using CST Microwave Studio 2016, each varactor was modeled with a series RLC equivalent circuit, which consists of R_s of 1.6 Ω, diode parasitic inductance (L_p) of 0.4 nH, parasitic capacitance (C_p) of 0.06 pF, and C_j as given in Table 3 [46], [47].

B. PROTOTYPES FABRICATION

The antenna was fabricated layer by layer, starting from the bottom to the top encapsulation layer for ease of integration of the antenna parts (Fig. 11). The same principle was applied when fabricating the rectangular samples and the transmission lines described in Section II. To achieve good PDMS-PDMS layer bonding, PDMS solution was directly poured and cured over a cured PDMS layer when making the multilayer PDMS structure [48]. The curing of each PDMS layer, including the PDMS-ceramic composite, was done in
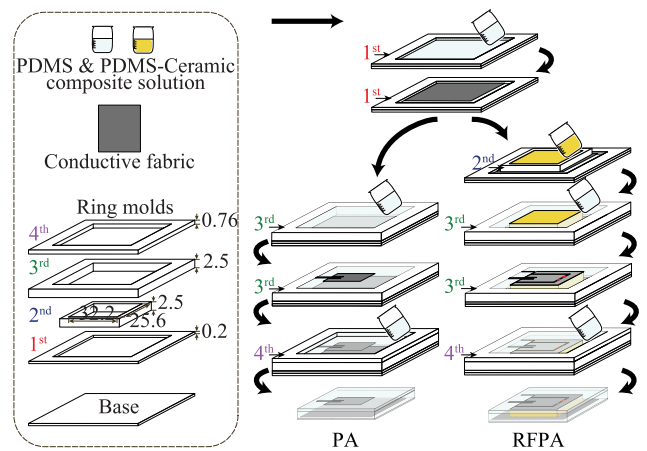
FIGURE 11. Schematic illustration of the fabrication process of the PDMS-embedded conductive fabric antennas.
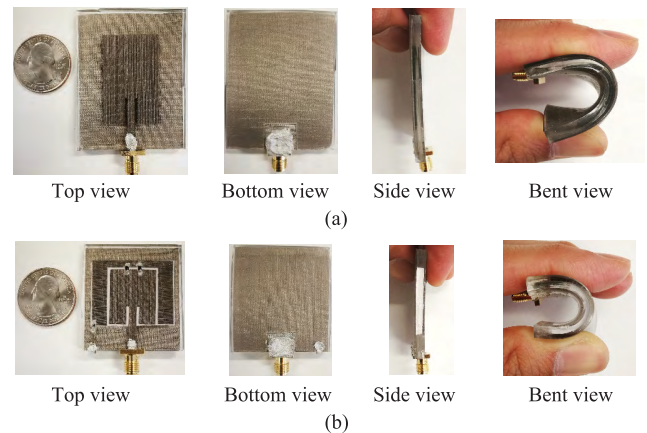
FIGURE 12. Fabricated prototypes. (a) PA. (b) RFPA.

the oven at 65°C for two hours, while for the thin PDMS layers that were used to attach the conductive fabric, it was done with 80°C temperature for only 30 minutes. Before curing in the oven, the solutions were always degassed in a vacuum desiccator for about 40 minutes to remove air bubbles trapped inside.

Taking advantage of the initial liquid state of PDMS, we used customized ring-shaped molds made out of commercial laminates from Taconic having the thicknesses required by the designs, into which we can pour the PDMS solution and guarantee the accuracy of the thickness of each layer. To make the mold, a rectangular aperture that is big enough to contain the designs were made on each laminate. Only for the second mold that was used to make the PDMS-ceramic composite substrate, the width and length of the aperture were precisely made following the area of the radiator patches to ensure that the size of the composite substrate fits the area of the radiating patches. As can be seen in the fabrication flow, once the composite substrate was cured, the second mold was removed before proceeding to the next PDMS layer.

The top and bottom encapsulation layers were cut slightly at the edges of the transmission lines and the bias line of the RFPA, to be able to attach SMA connectors and a short copper wire connecting the bias line to the ground plane for measurement purposes. The attachment was done by means of silver epoxy, and to cure it the antenna was left again in the oven at 65°C for another one hour. The same treatment was done for attaching the varactors and inductor on the RFPA. Photographs of the fabricated PDMS-embedded conductive fabric antennas are shown in Figs. 12(a) and (b).

IV. MEASUREMENTS AND TESTING

Next, we proceeded to characterize the RF performance of the fabricated antennas in both free space and the on-body environment. The latter was done with UWB semisolid phantoms as shown in Figs. 13(a), (b), and (c), for assessing two critical aspects of wearable antennas i.e. the performance in the vicinity of a human body and the influence of physical deformation. The phantoms, prepared following the procedure in [49], have the electrical properties as shown in Fig. 14, which agree very well with those of a human muscle reported in [50]. During the measurements with the flat phantom, a gap of 5 mm was maintained between the antennas and the phantom using foam to emulate the actual placement of the antenna on a human body with clothing.

A. $|S_{11}|$

As shown in Figs. 15(a) and (b), the measured $|S_{11}|$ parameters of both antennas are largely in accord with the simulations. Using the adjusted conductivity values, a better agreement between the measured and simulated results compared with those previously shown in [28] can be noticed. In free space, the patch antenna has 10 dB return-loss bandwidth of 3.3% centered at 2.45 GHz, while the reconfigurable patch antenna demonstrates resonance-frequency tuning from 2.37 to 2.66 GHz with an average 10 dB return-loss bandwidth of 3.7%. When placed in close proximity to the flat phantom as illustrated in Fig. 13(a), the changes in the $|S_{11}|$ of both antennas are insignificant (see Figs. 16(a) and (b)), thanks to the antenna-phantom isolation provided by the ground plane.

B. ROBUSTNESS AGAINST PHYSICAL DEFORMATION

To investigate the effect of physical deformation on the antenna performance, we severely bent each antenna in its E and H-planes around the phantom's wrist having a radius of 28 mm, as illustrated in Figs. 13(c). As expected, due to the significant alteration in the main current path of the antennas, the bending in their E-plane has a major effect on the resonance-frequency shift, whereas bending in the H-plane has a negligible effect on the antenna input impedance and resonance frequency (see Figs. 16(a) and (b)). Therefore, in practice it is normally suggested to avoid bending the antenna in the E-plane [51]. However, this is not a problem in the active design where the resonance frequency can be retuned easily by adjusting the bias voltage. It should be noted
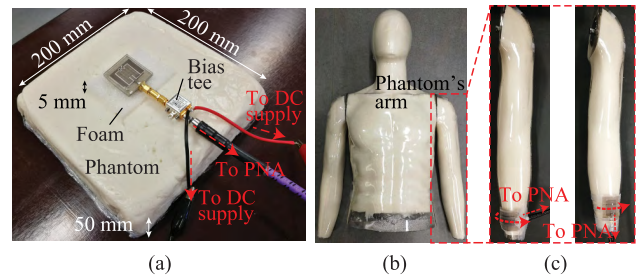

FIGURE 13. Experimental setup for $|S_{11}|$ measurements on phantoms. (a) RFPA mounted on the flat phantom. (b) Torso phantom for bending tests. (c) PA wrapped on the phantom's wrist with E-plane (left) and H-plane (right) bendings.
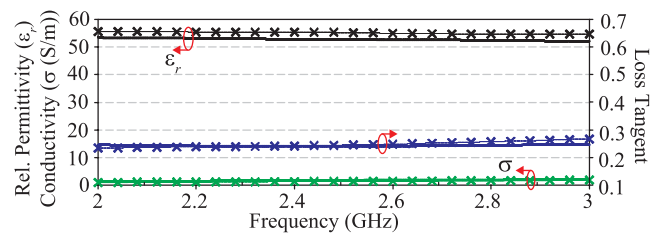

FIGURE 14. Measured (solid lines with cross markers) electrical properties of the fabricated UWB phantoms compared to the reference data [50] (solid lines).
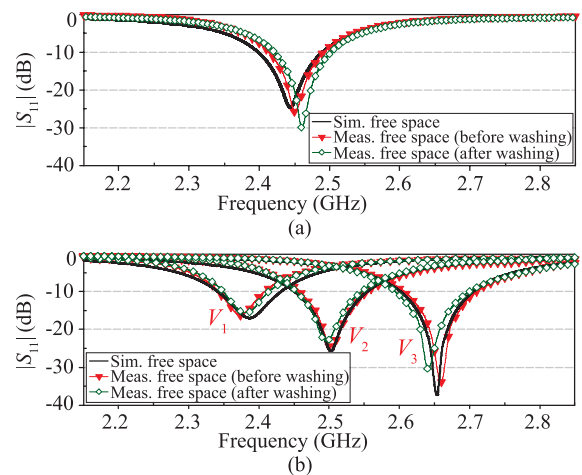
FIGURE 15. $|S_{11}|$ of the antenna in free space. (a) PA. (b) RFPA.

that, due to the flexibility of the combined PDMS or PDMS composite and conductive fabric, the antennas can be bent easily to a radius of less than 28 mm, and still return to their original shape. The PDMS encapsulation also seals the lumped components firmly on the antenna radiator surface, thus maintaining the reconfigurability even under severe bending.

C. RESILIENCE TO EXTREME ENVIRONMENT

The resilience of the proposed fabrication method was further assessed through a washability test. Both the antennas were washed in a household washing machine together with other laundry using detergent, bleach, and 40°C water

FIGURE 16. $|S_{11}|$ of the antenna on the flat phantom and under bending on the phantom's wrist. (a) PA. (b) RFPA.
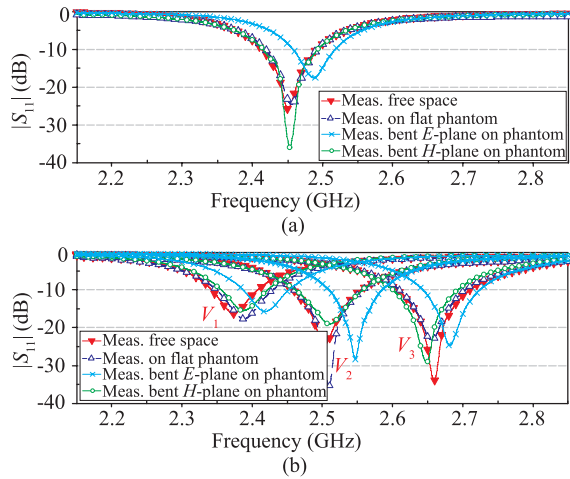

Sim. co-pol free space
Sim. x-pol free space
Meas. co-pol free space
Meas. x-pol free space
Meas. co-pol on flat phantom
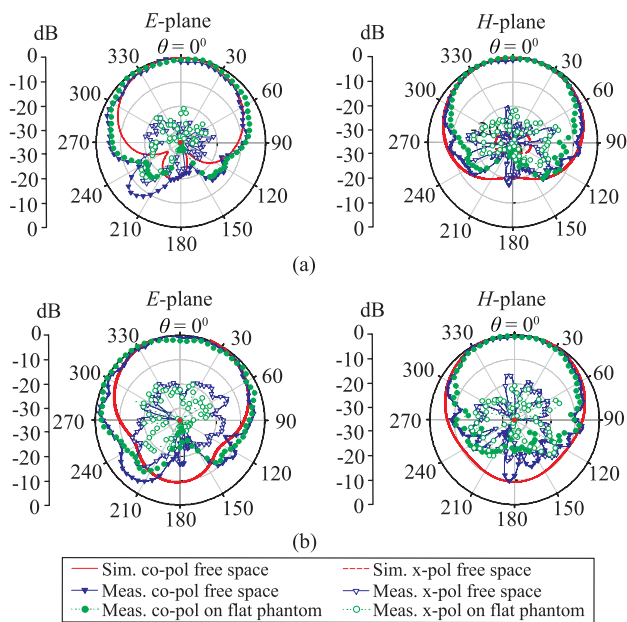Meas. x-pol on flat phantom

FIGURE 17. Normalized simulated and measured radiation patterns of the antennas in free space and on the flat phantom. (a) PA. (b) RFPA at State II.

TABLE 4. Summary of the peak gains and efficiencies of the prototypes fabricated with PDMS-embedded conductive fabric.

Result	PA		RFPA*	
	Gain (dBi)	Eff. (%)	Gain (dBi)	Eff. (%)
Sim. free space	1.7	35	0.6 to 1.4	29 to 40
Meas. free space	1.6	34	0.4 to 1.3	28 to 39
Meas. on flat phantom	1.1	27	−1.1 to 0.3	17 to 19

*The results over the entire tuning range (0 to 20 V bias voltage)

in one complete cycle for around 45 minutes. Each connector of the antennas was sealed with a plastic cap and tape to minimize water exposure and to protect the connection against turbulence inside the machine. Once dry, the

TABLE 5. Previously reported flexible wearable antennas.

Antenna	Freq. (MHz)	Tot. efficiency (%)	
		In free space	On body
[8]	2450	31 − 41	NA
[9]	1800 − 3000	76 − 86	33 − 63
[10]	383.5	25*	NA
[12]	2920	41.5	NA
[13]	2450/5200	40/40	NA
[14]	2400	37	NA
[15]	2490/2670/4520	15.2/14.3/41.4	NA
[17]	2450	81	60
[18]	2450	24	14
[26]	2450	3.3	NA
[27]	915/1575	NA	6.39/72.6
[29]	2450	NA	27

*Simulated result only

$|S_{11}|$ parameters of both antennas were re-measured. As can be seen in Figs. 15(a) and (b), no significant discrepancies appear in the $|S_{11}|$ of both antennas. The minor changes are found to be caused by the SMA to antenna connection that was flexed slightly due to the turbulence inside the washing machine. Most importantly, an almost identical reconfigurability performance before and after washing is shown by the RFPA. These results validate the superiority of the proposed method. The PDMS encapsulation keeps the conductive parts of the antenna as well as the lumped elements from being detached during washing and also protects them from water or any other chemical exposure. Consequently, a well-preserved antenna efficiency can be expected, since PDMS prevents the dissolution of the fabric's conductive materials [19].

D. RADIATION PERFORMANCE

The normalized radiation patterns of PA and RFPA, in free space and when mounted on the flat phantom, are given in Figs. 17(a) and (b). The patterns are shown at the free-space resonance frequency of PA and RFPA operating at State II. As expected from a patch antenna operating in its fundamental mode, the maximum radiation is in the broadside direction. For the RFPA, the patterns are quite stable over the entire tuning range. However, for brevity, only the pattern at State II is shown. The on-phantom radiation patterns generally appear to be quite similar to those in free space, apart from the slight decrease in the back radiation.

Table 4 summarizes the peak gains and efficiencies of both antennas. A good agreement is shown between the simulated and measured results in free space, which once again validates the accurate estimation of the fabric conductivity after being embedded in PDMS. The gains and efficiencies are decreased when the antennas are placed on the phantom. However, these decrements can be considered

low for antennas having a relatively small ground plane with an imperfect conductivity. Compared to our work presented in [28], the current reconfigurable prototype has a maximum 2.5 dB lower gain in free space, which is expected as the consequence of the conductive-fabric selection and the inclusion of the PDMS-ceramic composite. Nonetheless, in addition to the significantly smaller size, it demonstrates better robustness against physical deformation, thanks to the right conductive fabric combination. It can also be seen from Table 5 that the efficiencies of the antennas fabricated with PDMS-embedded conductive fabric are still comparable to some previously reported flexible wearable antennas realized with other techniques.

V. CONCLUSION

We have demonstrated a practical approach to achieve robustness with flexibility in wearable antennas. Conductive fabric embedded within PDMS polymer was thoroughly characterized. Antennas were fabricated using this method, and their RF performance including reconfigurability was studied by exposing the antennas to various deformations and harsh test environments. Excellent performance was obtained, consistently, even after washing the antennas in a machine, validating the applicability of the proposed approach for realization of robust flexible antennas or other RF electronic components for wearable applications. Moreover, the good agreement between the simulated and measured results adds further assurance to the analysis and shows that the materials and methods involved allow reliable antenna optimization using regular modeling approaches. As future work, some possibilities to improve the efficiency of the PDMS-embedded conductive fabric based antennas will be examined. These include repetitive coating of the conductive fabric with certain conductive materials to increase the effective conductivity of the fabric [4] and mixing PDMS with micro/nanoparticles such as alumina, polytetrafluoroethylene (PTFE), and glass microspheres to reduce the loss of PDMS [52]–[54]. The effect of these methods on the mechanical properties of both materials and thus the mechanical robustness of the PDMS-embedded conductive fabric will also be investigated. In addition, a multiple washing test to further verify the washability and hence the robustness of the proposed method will be conducted in the near future.

REFERENCES

[1] S. Koulouridis, G. Kiziltas, Y. Zhou, D. J. Hansford, and J. L. Volakis, "Polymer–ceramic composites for microwave applications: Fabrication and performance assessment," *IEEE Trans. Microw. Theory Techn.*, vol. 54, no. 12, pp. 4202–4208, Dec. 2006.

[2] Y. Ouyang and W. J. Chappell, "High frequency properties of electro-textiles for wearable antenna applications," *IEEE Trans. Antennas Propag.*, vol. 56, no. 2, pp. 381–389, Feb. 2008.

[3] Y. Zhou, Y. Bayram, F. Du, L. Dai, and J. L. Volakis, "Polymer-carbon nanotube sheets for conformal load bearing antennas," *IEEE Trans. Antennas Propag.*, vol. 58, no. 7, pp. 2169–2175, Jul. 2010.

[4] Y. Bayram *et al.*, "E-textile conductors and polymer composites for conformal lightweight antennas," *IEEE Trans. Antennas Propag.*, vol. 58, no. 8, pp. 2732–2736, Aug. 2010.

[5] Z. Wang, L. Zhang, Y. Bayram, and J. L. Volakis, "Multilayer printing of embroidered RF circuits on polymer composites," in *Proc. IEEE Int. Symp. Antennas Propag. (APSURSI)*, Jul. 2011, pp. 278–281.

[6] M. L. Scarpello *et al.*, "Design of an implantable slot dipole conformal flexible antenna for biomedical applications," *IEEE Trans. Antennas Propag.*, vol. 59, no. 10, pp. 3556–3564, Oct. 2011.

[7] S. Kim, Y.-J. Ren, H. Lee, A. Rida, S. Nikolaou, and M. M. Tentzeris, "Monopole antenna with inkjet-printed EBG array on paper substrate for wearable applications," *IEEE Antennas Wireless Propag. Lett.*, vol. 11, pp. 663–666, 2012.

[8] M. L. Scarpello, I. Kazani, C. Hertleer, H. Rogier, and D. V. Ginste, "Stability and efficiency of screen-printed wearable and washable antennas," *IEEE Antennas Wireless Propag. Lett.*, vol. 11, pp. 838–841, 2012.

[9] P. J. Soh, G. A. E. Vandenbosch, S. L. Ooi, and N. H. M. Rais, "Design of a broadband all-textile slotted PIFA," *IEEE Trans. Antennas Propag.*, vol. 60, no. 1, pp. 379–384, Jan. 2012.

[10] J. Trajkovikj, J.-F. Zürcher, and A. K. Skrivervik, "PDMS, a robust casing for flexible W-ban antennas [EurAAP Corner]," *IEEE Antennas Propag. Mag.*, vol. 55, no. 5, pp. 287–297, Oct. 2013.

[11] B. Ivsic, D. Bonefacic, and J. Bartolic, "Considerations on embroidered textile antennas for wearable applications," *IEEE Antennas Wireless Propag. Lett.*, vol. 12, pp. 1708–1711, Dec. 2013.

[12] L. Song, A. C. Myers, J. J. Adams, and Y. Zhu, "Stretchable and reversibly deformable radio frequency antennas based on silver nanowires," *ACS Appl. Mater. Interfaces*, vol. 6, no. 6, pp. 4248–4253, 2014.

[13] S. Yan, P. J. Soh, and G. A. E. Vandenbosch, "Low-profile dual-band textile antenna with artificial magnetic conductor plane," *IEEE Trans. Antennas Propag.*, vol. 62, no. 12, pp. 6487–6490, Dec. 2014.

[14] W. G. Whittow *et al.*, "Inkjet-printed microstrip patch antennas realized on textile for wearable applications," *IEEE Antennas Wireless Propag. Lett.*, vol. 13, pp. 71–74, Jan. 2014.

[15] J. Tak and J. Choi, "An all-textile Louis Vuitton logo antenna," *IEEE Antennas Wireless Propag. Lett.*, vol. 14, pp. 1211–1214, 2015.

[16] S. Wang, N. L. Chong, J. Virkki, T. Björninen, L. Sydänheimo, and L. Ukkonen, "Towards washable electrotextile UHF RFID tags: Reliability study of epoxy-coated copper fabric antennas," *Int. J. Antennas Propag.*, vol. 2015, Nov. 2015, Art. no. 424150.

[17] S. Agneessens, S. Lemey, T. Vervust, and H. Rogier, "Wearable, small, and robust: The circular quarter-mode textile antenna," *IEEE Antennas Wireless Propag. Lett.*, vol. 14, pp. 1482–1485, 2015.

[18] J. Tak, S. Lee, and J. Choi, "All-textile higher order mode circular patch antenna for on-body to on-body communications," *IET Microw., Antennas Propag.*, vol. 9, no. 6, pp. 576–584, Apr. 2015.

[19] Y. Y. Fu *et al.*, "Experimental study on the washing durability of electro-textile UHF RFID tags," *IEEE Antennas Wireless Propag. Lett.*, vol. 14, pp. 466–469, 2015.

[20] S. Pacchini *et al.*, "Inkjet-printing of hybrid Ag/conductive polymer towards strechable microwave devices," in *Proc. Eur. Microw. Conf. (EuMC)*, Sep. 2015, pp. 865–868.

[21] G.-W. Huang, H.-M. Xiao, and S.-Y. Fu, "Wearable electronics of silver-nanowire/poly(dimethylsiloxane) nanocomposite for smart clothing," *Sci. Rep.*, vol. 5, no. 2, 2015, Art. no. 13971.

[22] A. Kiourti, J. L. Volakis, R. B. V. B. Simorangkir, S. M. Abbas, and K. P. Esselle, "UWB antennas on conductive textiles," in *Proc. IEEE Int. Symp. Antennas Propag. (APSURSI)*, Jun. 2016, pp. 1941–1942.

[23] S. J. Chen, T. Kaufmann, D. C. Ranasinghe, and C. Fumeaux, "A modular textile antenna design using snap-on buttons for wearable applications," *IEEE Trans. Antennas Propag.*, vol. 64, no. 3, pp. 894–903, Mar. 2016.

[24] X. Huang *et al.*, "Highly flexible and conductive printed graphene for wireless wearable communications applications," *Sci. Rep.*, vol. 5, no. 1, 2016, Art. no. 18298.

[25] R. B. V. B. Simorangkir, Y. Yang, L. Matekovits, and K. P. Esselle, "Dual-band dual-mode textile antenna on PDMS substrate for body-centric communications," *IEEE Antennas Wireless Propag. Lett.*, vol. 16, pp. 677–680, 2017.

[26] M. Rizwan, M. W. A. Khan, L. Sydänheimo, J. Virkki, and L. Ukkonen, "Flexible and stretchable brush-painted wearable antenna on a three-dimensional (3-D) printed substrate," *IEEE Antennas Wireless Propag. Lett.*, vol. 16, pp. 3108–3112, 2017.

[27] H. Lee, J. Tak, and J. Choi, "Wearable antenna integrated into military berets for indoor/outdoor positioning system," *IEEE Antennas Wireless Propag. Lett.*, vol. 16, pp. 1919–1922, 2017.

[28] R. B. V. B. Simorangkir, Y. Yang, K. P. Esselle, and B. A. Zeb, "A method to realize robust flexible electronically tunable antennas using polymer-embedded conductive fabric," *IEEE Trans. Antennas Propag.*, vol. 66, no. 1, pp. 50–58, Jan. 2018.

[29] H. Li, S. Sun, B. Wang, and F. Wu, "Design of compact single-layer textile MIMO antenna for wearable applications," *IEEE Trans. Antennas Propag.*, vol. 66, no. 6, pp. 3136–3141, Jun. 2018.

[30] I. D. Johnston, D. K. McCluskey, C. K. L. Tan, and M. C. Tracey, "Mechanical characterization of bulk Sylgard 184 for microfluidics and microengineering," *J. Micromech. Microeng.*, vol. 24, no. 3, pp. 035017-1–035017-7, 2014.

[31] N. Tiercelin, P. Coquet, R. Sauleau, V. Senez, and H. Fujita, "Poly-dimethylsiloxane membranes for millimeter-wave planar ultra flexible antennas," *J. Micromech. Microeng.*, vol. 16, no. 11, pp. 2389–2395, 2006.

[32] A. Colas, "Silicones: Preparation, properties and performances," *Soc. Roy. Chimie*, vol. 8, no. 30, pp. 847–852, 1990.

[33] M. T. Sebastian and L. K. Namitha, "Rubber–ceramic composites," in *Microwave Materials and Applications 2V Set*. Hoboken, NJ, USA: Wiley, 2017, pp. 537–574.

[34] P. Bodö and J.-E. Sundgren, "Titanium deposition onto ion-bombarded and plasma-treated polydimethylsiloxane: Surface modification, interface and adhesion," *Thin Solid Films*, vol. 136, no. 1, pp. 147–159, 1986.

[35] G. J. Hayes, J.-H. So, A. Qusba, M. D. Dickey, and G. Lazzi, "Flexible liquid metal alloy (EGaIn) microstrip patch antenna," *IEEE Trans. Antennas Propag.*, vol. 60, no. 5, pp. 2151–2156, May 2012.

[36] Y. Tao, Y. Tao, L. Wang, B. Wang, Z. Yang, and Y. Tai, "High-reproducibility, flexible conductive patterns fabricated with silver nanowire by drop or fit-to-flow method," *Nanoscale Res. Lett.*, vol. 8, no. 1, p. 147, 2013.

[37] A. Kamyshny and S. Magdassi, "Conductive nanomaterials for printed electronics," *Small*, vol. 10, no. 17, pp. 3515–3535, 2014.

[38] A. Kiourti and J. L. Volakis, "Stretchable and flexible E-fiber wire antennas embedded in polymer," *IEEE Antennas Wireless Propag. Lett.*, vol. 13, pp. 1381–1384, 2014.

[39] S. Shao, A. Kiourti, R. J. Burkholder, and J. L. Volakis, "Broadband textile-based passive UHF RFID tag antenna for elastic material," *IEEE Antennas Wireless Propag. Lett.*, vol. 14, pp. 1385–1388, 2015.

[40] P. L. Wise, I. M. Reaney, W. E. Lee, T. J. Price, D. M. Iddles, and D. S. Cannell, "Structure-microwave property relations of Ca and Sr titanates," *J. Eur. Ceram. Soc.*, vol. 21, no. 15, pp. 2629–2632, 2001.

[41] S. Rajesh, K. P. Murali, K. V. Rajani, and R. Ratheesh, "SrTiO$_3$-filled PTFE composite laminates for microwave substrate applications," *Int. J. Appl. Ceram. Tech.*, vol. 6, no. 5, pp. 553–561, 2009.

[42] Z. Xu, T. Kaufmann, and C. Fumeaux, "Wearable textile shielded stripline for broadband operation," *IEEE Microw. Compon. Lett.*, vol. 24, no. 8, pp. 566–568, Aug. 2014.

[43] K.-P. Lätti, M. Kettunen, J.-P. Ström, and P. Silventoinen, "A review of microstrip T-resonator method in determining the dielectric properties of printed circuit board materials," *IEEE Trans. Instrum. Meas.*, vol. 56, no. 5, pp. 1845–1850, Oct. 2007.

[44] R. Garg, R. Bhartia, I. Bahl, and A. Ittipiboon, "Rectangular microstrip antennas," in *Microstrip Antenna Design Handbook*. Boston, MA, USA: Artech House, 2001, ch. 4, p. 265.

[45] W.-Y. Zhou, S.-H. Qi, H.-Z. Zhao, and N.-L. Liu, "Thermally conductive silicone rubber reinforced with boron nitride particle," *Polym. Compos.*, vol. 28, no. 1, pp. 23–28, 2007.

[46] A. R. Weily, T. S. Bird, and Y. J. Guo, "A reconfigurable high-gain partially reflecting surface antenna," *IEEE Trans. Antennas Propag.*, vol. 56, no. 11, pp. 3382–3390, Nov. 2008.

[47] Aeroflex Microelectronic Solutions. *GaAs Hyperabrupt Varactor Diodes MGV Series, A17041 Datasheet*, 2005. [Online]. Available: http://www.aeroflex-metelics.com

[48] M. A. Eddings, M. A. Johnson, and B. K. Gale, "Determining the optimal PDMS–PDMS bonding technique for microfluidic devices," *J. Micromech. Microeng.*, vol. 18, no. 6, p. 067001, Jun. 2008.

[49] K. Ito, K. Furuya, Y. Okano, and L. Hamada, "Development and characteristics of a biological tissue-equivalent phantom for microwaves," *Electron. Commun. Jpn. I, Commun.*, vol. 84, no. 4, pp. 67–77, 2001.

[50] D. Andreuccetti, R. Fossi, and C. Petrucci, "An Internet resource for the calculation of the dielectric properties of body tissues in the frequency range 10 Hz–100 GHz," IFAC-CNR, Florence, Italy, Tech. Rep., 1997. [Online]. Available: http://niremf.ifac.cnr.it/tissprop/

[51] T. Kellomäki, "Analysis of circular polarization of cylindrically bent microstrip antennas," *Int. J. Antennas Propag.*, vol. 2012, May 2012, Art. no. 85031.

[52] D. Headland *et al.*, "Modified elastomeric polymers for loss reduction in the terahertz range," in *Proc. 40th Int. Conf. Infr., Millim., Terahertz Waves (IRMMW-THz)*, Aug. 2015, pp. 1–2.

[53] D. Headland *et al.*, "Doped polymer for low-loss dielectric material in the terahertz range," *Opt. Mater. Express*, vol. 5, no. 6, pp. 1373–1380, Jun. 2015.

[54] W. A. W. Muhamad, R. Ngah, M. F. Jamlos, P. J. Soh, and M. T. Ali, "High-gain dipole antenna using polydimethylsiloxane–glass microsphere (PDMS-GM) substrate for 5G applications," *Appl. Phys. A, Solids Surf.*, vol. 123, no. 1, p. 102, Jan. 2016.
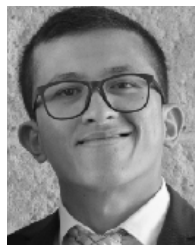
ROY B. V. B. SIMORANGKIR (S'15) received the B.S. degree in telecommunication engineering from the Bandung Institute of Technology, Bandung, Indonesia, in 2010, the M.S. degree in electrical and electronic engineering from Yonsei University, Seoul, South Korea, in 2014, and the Ph.D. degree in electronic engineering from Macquarie University, Sydney, NSW, Australia, in 2018.

From 2010 to 2012, he was a Lecturer with the Electrical Engineering Department, Institut Teknologi Harapan Bangsa, Bandung, Indonesia. He received the Korean Government Scholarship during master's studies and an International Macquarie Research Excellence Scholarship (iMQRES) for Ph.D. studies. His general research interests include flexible wearable antennas, reconfigurable antennas, ultra-wideband antennas, and leaky wave antennas.

Dr. Simorangkir was selected as a finalist in the Student Paper and Advance Practice Paper Competitions of the 2017 IEEE MTT-S International Microwave Symposium, Honolulu, HI, USA. He also received the First Price in the 2017 IEEE Region 10 Student Paper Contest, postgraduate category.
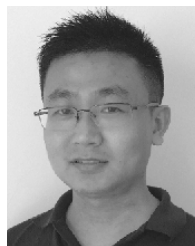
YANG YANG (S'11–M'14–SM'17) was born in Bayan Nur, China. He received the Ph.D. degree from Monash University, Melbourne, VIC, Australia, in 2013. From 2012 to 2015, he was an Asia Pacific GSP Engineer at Rain Bird and a Global GSP Success Award holder of the year 2014. From 2015 to 2016, he served as a Senior Research Associate with the Department of Engineering, Macquarie University, Sydney, NSW, Australia.

In 2016, he was a Research Fellow with the State Key Laboratory of Millimeter-Waves, City University of Hong Kong. In 2016, he has been involved in the National Basic Research Program of China (973 Program) and appointed as an Honorary Research Fellow with the Shenzhen Institute, City University of Hong Kong. In 2016, he joined the University of Technology Sydney, Australia, as a Lecturer. His research interests include RFIC, microwave and millimeter-wave circuits and systems, reconfigurable antennas, wearable antennas, and wearable medical sensing devices and systems. He is a current Associate Editor of IEEE Access.

RAHEEL M. HASHMI (S'12–M'15) received the B.S. degree (Hons.) from the COMSATS Institute of Information Technology, Islamabad, Pakistan, in 2009, the M.S. degree from the Politecnico di Milano, Milan, Italy, in 2011, and the Ph.D. degree from Macquarie University, Sydney, NSW, Australia, in 2015.

He held a research associate position at the Reconfigurable Electronics and Antennas Research Group, Macquarie University. He is currently a Lecturer with the School of Engineering, Macquarie University. He has authored over 40 refereed journal and conference publications. He is an inventor of two patent applications. His current research interests include EBG structures and their use in electromagnetic applications, EBG resonator antennas, FSS, wideband directive antennas, ultrawideband antennas, and antennas for biomedical applications.

Dr. Hashmi was a recipient of several prestigious awards and fellowships, including the URSI Young Scientist Award, the Commonwealth International Postgraduate Research Scholarship, the CSIRO OCE Ph.D. Fellowship, and the Institutes Gold Medal from the COMSATS Institute of Information Technology. He is the Chair of the IEEE Young Professionals Affinity Group, NSW, and the Secretary of the IEEE Antennas and Propagation/MTT Joint Chapter, NSW. He has been serving as an Associate Editor of the *IET Microwaves, Antennas and Propagation* since 2016.

TONI BJÖRNINEN (M'09–SM'18) received the M.Sc. and Ph.D. degrees in electrical engineering from the Tampere University of Technology (TUT), Tampere, Finland, in 2009 and 2012, respectively.

He is currently an Academy of Finland Research Fellow with the BioMediTech Institute and Faculty of Biomedical Sciences and Engineering, TUT. He has been a Visiting Post-Doctoral Scholar with the Berkeley Wireless Research Center, University of California at Berkeley and with the Microwave and Antenna Institute, Electronic Engineering Department, Tsinghua University, Beijing. His research focuses on technology for wireless health including implantable and wearable antennas and sensors, and RFID-inspired wireless solutions.

Dr. Björninen is an author of 148 peer-reviewed scientific publications. He serves as an Associate Editor of *IET Electronics Letters* and the IEEE JOURNAL OF RADIO FREQUENCY IDENTIFICATION.

KARU P. ESSELLE (M'92–SM'96–F'16) received the B.Sc. degree (Hons.) in electronic and telecommunication engineering from the University of Moratuwa, Sri Lanka, and the M.A.Sc. and Ph.D. degrees in electrical engineering from the University of Ottawa, Canada. He is a Professor of electronic engineering with Macquarie University, Sydney, the Director of the WiMed Research Centre (one of the two) and the Past Associate Dean–Higher Degree Research (HDR) of the Division of Information and Communication Sciences. He has also served as a member of the Dean's Advisory Council and the Division Executive and as the Head of the Department of Engineering, Macquarie University several times. In 2018, he has been selected to chair the prestigious Distinguished Lecturer Program Committee of the IEEE Antennas and Propagation (AP) Society—the premier global learned society dedicated for antennas and propagation—which has over 8000 members worldwide. After two stages in the selection process, he has been selected by this Society as one of two candidates in the ballot for 2019 President of the Society. Only three people from Asia or Pacific apparently have received this honour (one from Australia and two from Japan) in the 68-year history of this Society. He is also one of the three Distinguished Lecturers of the IEEE AP Society for 2017–2019. He is also one of the three Distinguished Lecturers (DL) selected by the Society in 2016. He is the only Australian to chair the AP DL Program ever, the only Australian AP DL in almost two decades, and second Australian AP DL ever. When he was elected to the IEEE AP Society Administrative Committee for a three-year term in 2014, he became the only person residing in the Asia-Pacific Region (IEEE Region 10) to be elected to this highly competitive position over a period of at least six years (2010–2015). He is also the Chair of the Board of Management of Australian Antenna Measurement Facility, and was the Elected Chair of both the IEEE New South Wales (NSW) Section and the IEEE NSW AP/MTT Chapter, in 2016 and 2017, respectively. He directs the Centre for Collaboration in Electromagnetic and Antenna Engineering. He was elevated to prestigious IEEE Fellow grade for his contributions to resonance-based antennas. He is also a fellow of Engineers Australia.

He has authored over 500 research publications and his papers have been cited more than 6900 times. He is the first Australian antenna researcher ever to reach Google Scholar h-index of 30 and his h-index is often the highest among Australian antenna researchers. Since 2002, his research team has been involved with research grants, contracts and Ph.D. scholarships worth over U.S. 16 million. His research has been funded by many national and international organizations, including the Australian Research Council, Intel, U.S. Air Force, Cisco Systems, Hewlett-Packard, and Australian and Indian governments.

He has been invited to serve as an international expert/research grant assessor by several nationwide research funding bodies overseas, including The Netherlands, Canada, Finland, Hong-Kong, Georgia, South Africa, and Chile. He has been invited by Vice-Chancellors of Australian and overseas universities to assess applications for promotion to professorial levels. He has also been invited to assess grant applications submitted to Australia's most prestigious schemes, such as the Australian Federation Fellowships and the Australian Laureate Fellowships. He leads the Implantable Wireless Program of the WiMed Research Centre. In addition to the large number of invited conference speeches he has given, he has been an invited keynote speaker of the IEEE workshops and conferences.

His awards include the 2017 Excellence in Research Award from the Faculty of Science and Engineering, the 2017 Engineering Excellence Award for Best Innovation, the 2017 Certificate of Recognition from IEEE Region 10, the 2016 and 2012 Engineering Excellence Awards for Best Published Paper from IESL NSW Chapter, the 2011 Outstanding Branch Counselor Award from IEEE headquarters (USA), the 2009 Vice Chancellor's Award for Excellence in Higher Degree Research Supervision, and the 2004 Innovation Award for Best Invention Disclosure. His mentees have been awarded many fellowships, awards, and prizes for their research achievements. Forty-five international experts who examined the theses of his recent Ph.D. graduates ranked them in the top 5

He has provided expert assistance to more than a dozen companies, including Intel, Santa Clara, CA, USA, Hewlett Packard Laboratory, Palo Alto, CA, USA, Cisco Systems, Richardson, TX, USA, Audacy, USA, Cochlear, Australia, Optus, Australia, ResMed, Australia, and Katherine-Werke, Rosenheim, Germany. He is an Associate Editor of the IEEE TRANSACTIONS ON ANTENNAS AND PROPAGATION and the IEEE ACCESS.

He is the Technical Program Committee Co-Chair of ISAP 2015, APMC 2011, and TENCON 2013 and the Publicity Chair of ICEAA 2016, IWAT 2014, and APMC 2000. His research activities are posted in the web at http://web.science.mq.edu.au/ esselle/.

LEENA UKKONEN (M'04) received the M.Sc. and Ph.D. degrees in electrical engineering from the Tampere University of Technology (TUT), Tampere, Finland, in 2003 and 2006, respectively.

She is currently a Professor and an Academy Research Fellow with the Faculty of Biomedical Science and Engineering, TUT, where she is leading the Wireless Identification and Sensing Systems Research Group.

● ● ●